Discover Oncology

Analysis

Multi-omics identify ribosome related causal genes methylation, splicing, and expression in prostate cancer

Chengcheng Wei[1] · Jingke He[1] · Yunfan Li[1] · Yu Luo[1] · Liangdong Song[1] · Kun Han[1] · Jindong Zhang[1] · Shuai Su[1] · Delin Wang[1]

Received: 4 January 2025 / Accepted: 5 May 2025
Published online: 12 May 2025

Abstract

Background Understanding the molecular underpinnings of prostate cancer remains a critical challenge in oncology. Ribosomes, essential cellular organelles responsible for protein synthesis, have emerged as potential regulators in cancer development. Previous studies suggest that dysfunction in ribosomal processes may contribute significantly to prostate cancer progression. We used summary-data-based Mendelian randomization (SMR) and colocalization analysis, as well as single-cell analysis, to investigate the association between ribosome-related genes and prostate cancer by integrating multi-omics.

Method In this study, we employed a multi-omics approach integrating genomics and transcriptomics data to investigate the role of ribosome-related genes in prostate cancer. Summary-level data for prostate cancer were obtained from The Prostate Cancer Association Group to Investigate Cancer Associated Alterations in the Genome and FinnGen studies. SMR analyses were performed to assess the relevance of ribosomal gene-related molecular signatures to prostate cancer. We further performed colocalization analysis to assess whether the identified signal pairs shared causal genetic variants. Genes were then validated with single-cell sequencing analysis.

Results We identified significant causal effects of ribosome gene methylation on prostate cancer. After integrating the multi-omics data of mQTL, sQTL and eQTL, we identified two ribosomal genes, NSUN4 and MPHOSPH6. Methylation and splicing at different sites on the NSUN4 gene showed increased and decreased risks for prostate cancer, indicating complex gene regulation mechanisms. For instance, NSUN4 methylation site of cg10215817 was genetically associated with the increased prostate cancer risk (OR 1.20, 95% CI 1.10,1.30), while NSUN4 methylation site of cg00937489 was genetically associated with the decreased prostate cancer risk (OR 0.84, 95% CI 0.74,0.94); NSUN4 chr1:46341497:46344801 splicing (OR 1.11, 95% CI 1.05–1.17) were positively associated with prostate cancer risk, while NSUN4 chr1:46340919:46344801 splicing (OR 0.95, 95% CI 0.92–0.97) were negatively associated with prostate cancer risk. Expression analysis indicated significant associations between prostate cancer risk and increased expression levels of NSUN4 (OR 1.06, 95% CI 1.03–1.09; PPH4 = 0.79) and MPHOSPH6 (OR 1.07, 95% CI 1.04–1.10; PPH4 = 0.70). In-depth single-cell analysis showed that NSUN4 highly expresses in epithelial cells, while MPHOSPH6 highly expresses in myeloid cells.

Conclusion The study found that ribosome NSUN4 and MPHOSPH6 genes were associated with prostate cancer risk. This integrative multi-omics study underscores the significance of ribosome-related genes in prostate cancer etiology. By

Chengcheng Wei, Jingke He, Yunfan Li and Yu Luo have contributed equally to this paper.

Supplementary Information The online version contains supplementary material available at https://doi.org/10.1007/s12672-025-02584-2.

✉ Jindong Zhang, zhangjindong@hospital.cqmu.edu.cn; ✉ Shuai Su, sushuai930809@163.com; ✉ Delin Wang, delinwang_cqmu@163.com | [1]Department of Urology, The First Affiliated Hospital of Chongqing Medical University, Chongqing, China.

elucidating the molecular mechanisms underlying ribosome dysfunction, our research identifies potential therapeutic targets for mitigating disease progression. These findings not only enhance our understanding of prostate cancer biology but also pave the way for personalized therapeutic strategies targeting ribosomal pathways to improve clinical outcomes.

Keywords Ribosome · Prostate cancer · Multi-omics · Summary-data-based Mendelian randomization (SMR) · Single cell analysis

1 Introduction

Prostate cancer is a major global health issue, being the second most common malignancy and the fifth leading cause of cancer mortality among men worldwide, also the most frequent malignancy and the second primary cause of cancer-related death in men in the United States [1, 2]. As is universally acknowledged, ribosomes are essential organelles for protein synthesis and are closely related to protein homeostasis [3, 4]. Ribosome dysfunction can result in abnormal protein accumulation, disrupting cellular functions and contributing to tumorigenesis [5, 6]. Mutations in ribosomal protein genes and alterations in ribosomal machinery are linked to various solid tumors, including prostate cancer [7, 8]. Ribosome dysfunction is crucial in prostate cancer pathogenesis, involving specific genes and molecular mechanisms. For example, various oncogenic signaling pathways converge on the ribosome, which collectively enhance protein synthesis and contribute to tumorigenesis in prostate cancer [9]. Elevated levels of ribosomal proteins, such as RPS2, are implicated in tumor development [10]. Additionally, ribosomal S6 kinase (RSK) can regulate transcription factors as well as RNA-binding factors, and is associated with cancer progression and resistance to endocrine therapy in prostate cancer [11, 12]. A RSK inhibitor PMD-026 can suppress the advancement of castration resistant adenocarcinoma. [13] Moreover, studies have shown that increased Sirtuin 7 levels can lead to increased prostate-specific antigen levels, elevated Gleason scores, metastasis, and drug resistance [14, 15]. In addition, research has also investigated ribosome-targeted therapies for cancers, including prostate cancer [9, 16]. These findings highlight ribosomal dysfunction and related genes as significant contributors to prostate cancer, offering potential therapeutic targets. However, the ribosome-related genes and their effects are unclear. Also, the methods used in these studies did not consider the impact of confounding factors to distinguish cause from effect.

Given the connection of ribosomal dysfunction of prostate cancer, we employ Mendelian Randomization (MR) analysis to discern the genetic determinants behind this association and explore their potential causal roles. MR analysis is a method that utilizes genetic variants as instrumental variables to infer that observed association between an exposure and an outcome is consistent with a causal effect [17]. Compared with observational studies, this approach has a lower likelihood of confounding and reverse causality bias, while minimizing the effects of lifestyle and environmental factors due to the random assignment of genetic variants at conception, which remain unaffected during disease progression [18]. A genome wide MR analysis identified mitochondrial-related genes causally associated with multiple cancers [19]. Another MR analysis identified MTHFD1 and LGALS4 with increased risk of prostate adenocarcinoma [20]. The increasing number of extensive GWAS databases integrated with gene methylation, splicing, and expression quantitative trait loci (mQTL, sQTL, and eQTL) data enables the investigation of causal links between the regulation of ribosome-related genes and prostate cancer, considering methylation, splicing and expression [21].

To our knowledge, no MR studies have investigated the potential causal relationship between ribosomal dysfunction and prostate cancer risk. In this study, we applied a summary-data-based Mendelian randomization (SMR) using a multi-omics approach, along with single-cell sequencing, to examine the potential connections between ribosomal gene methylation, splicing, as well as expression and the risk of developing prostate cancer. This study aims to investigate the causal relationship between genetically driven ribosome dysfunction and prostate cancer using SMR and single-cell sequencing.

2 Methods

Figure 1 illustrates the overall design of the study. Our MR analysis utilized publicly available datasets, including The Prostate Cancer Association Group to Investigate Cancer Associated Alterations in the Genome (PRACTICAL) and FinnGen studies, as well as other large-scale GWAS data. In our analysis, we extracted instrumental variables of ribosomal genes across methylation, splicing and expression levels. MR analyses of prostate cancer were subsequently conducted separately at different biological levels. Colocalization analysis was subsequently applied to enhance causal inference. The PRACTICAL dataset was used in the discovery phase, while the FinnGen dataset was employed for replication to validate our findings. Furthermore, single-cell sequencing analysis was conducted using data sourced from the Gene Expression Omnibus (GEO) database to illustrate the expression of genes in individual cells. By integrating findings obtained from the three different levels of MR analysis and single cell sequencing, we identified several potential causal candidate genes.

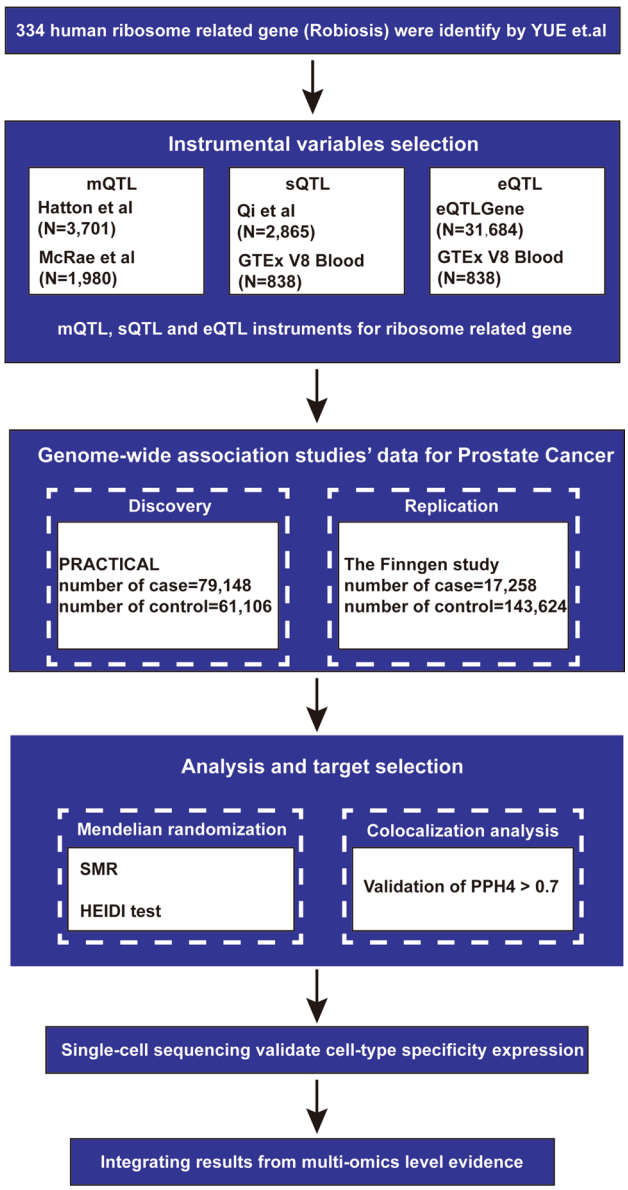

Fig. 1 Flowchart of Study

2.1 Data sources of methylation, splicing, and expression QTLs

QTLs can uncover the relationships between single nucleotide polymorphisms (SNPs) and variations in gene methylation, splicing, as well as expression. The associations of SNP-CpG in blood samples were derived from the mQTL dataset by Hatton et al. [22] and McRae et al. [23, 24] in 3710 and 1980 European ancestry individuals respectively.

The dataset of gene sQTL was collected from BrainMeta v2 cis-sQTL summary data with 2865 samples [25], and the V8 release of the GTEx sQTL summary data with 838 individuals [26]. The blood eQTL dataset was sourced from the eQTLGen consortium, including data from 31,684 individuals [27], and the V8 release of the GTEx eQTL summary data (n = 838) [26].

Ribosomal-related genes were identified by a list of 331 human mitochondrial genes [28]. Yue et al. found these genes in the mitochondrion, guided by the GO term from MSigDB and the descriptions provided by Nerurkar et al. [29]. Utilizing the inventory, ribosomal genes were separately identified within the QTL datasets. (Table S1).

2.2 Prostate cancer outcome datasets

Summary-level data for prostate cancer were obtained from PRACTICAL and FinnGen studies. Participants from PRACTICAL included a total of 79,148 cases and 61,106 controls [30]. Summary data for genetic associations with prostate cancer were downloaded from the public R11 release of the FinnGen study, including 17,258 cases and 143,624 control subjects in total [31]. The PRACTICAL dataset was used for the discovery phase of the study, whereas the replication phase employed data from the FinnGen study. All participants in both datasets were of European ancestry, and there was no sample overlap between the two datasets.

2.3 Summary-data-based MR analysis

Summary-data-based Mendelian randomization (SMR) was employed to assess the association between methylation, splicing, and expression of mitochondrial genes and the risk of prostate cancer. SMR provides significantly higher statistical power than traditional MR analysis, especially when utilizing top associated cis-QTLs and when both exposure and outcome information originate from two large-scale, distinct population [32]. In this study, we selected the most strongly associated cis-QTLs by defining a window centered on each gene (± 1000 kb) and applying a P-value threshold of 5.0×10^{-8}. SNPs with allele frequency differences greater than 0.2 between any dataset pair—such as the linkage disequilibrium (LD) reference sample, QTL summary data, and outcome summary data—were excluded. Colocalization was assessed using the heterogeneity in the dependent instrument (HEIDI) test, which relies on an external reference to differentiate pleiotropy from linkage disequilibrium. SNPs with a P-HEIDI value less than 0.01 were regarded as potentially pleiotropic and were therefore excluded from further analysis. The SMR and HEIDI tests were conducted using SMR software (version 1.3.1). We controlled the false discovery rate (FDR) at $\alpha = 0.05$ through the Benjamini–Hochberg method, considering associations for colocalization analysis if they met both an FDR-adjusted P-value threshold of < 0.05 and a P-HEIDI value > 0.01.

2.4 Colocalization analysis

Colocalization analyses were performed to identify shared causal variants between prostate cancer and identified ribosomal-related QTLs using the R package "coloc." In our study, several distinct posterior probabilities were found, each one matching an exclusive hypothesis: (1) absence of causal variants for both traits (H0); (2) presence of a causal variant influencing only gene expression (H1); (3) presence of a causal variant affecting only disease risk (H2); (4) separate causal variants for each trait (H3); and (5) a shared causal variant influencing both traits (H4).

In cancer GWAS databases, every primary SNP is followed by retrieval of all SNPs within 1000 kb, 1000 kb and 500 kb range both upstream and downstream for colocalization analysis of mQTL-GWAS, sQTL-GWAS, and eQTL-GWAS. This analysis focused on the posterior probability of H4 (PPH4), where a PPH4 value larger than 0.7 was defined as the threshold to determine significant colocalization between GWAS and QTL associations [33].

2.5 Single cell sequencing

Prostate cancer samples (a total of 14,985 cells) were obtained from the single-cell RNA sequencing dataset (GSE221603) in the GEO database. The single-cell RNA sequencing data were then processed using the "Seurat" R package. To ensure

high-quality data for single-cell RNA expression, a preliminary quality control assessment was performed using the following filtering criteria: (1) UMI counts of each cell sequenced was greater than 1000, with the top 3% of cells were removed; (2) cells with < 300 or > 7000 measured genes were excluded; and (3) cells with mitochondrial contamination > 10% or erythrocyte contamination greater than 3% were excluded. After quality control, a total of 14,985 high-quality cell samples were isolated from tissues of various different types of prostate cancer for further analysis. The data were then normalized using the "NormalizeData" function with Harmony selected for batch correction and integration. Principal component analysis (PCA) was used for preliminary dimensionality reduction of the data. Subsequently, we then applied uniform manifold approximation and projection (UMAP) and t-distributed stochastic neighbor embedding (t-SNE) algorithms to perform dimensionality reduction and clustering visualization of high-dimensional single-cell RNA sequencing data. Finally, the UMAP clustering method was chosen, dividing the cells into 12 different clusters.

2.6 Integration of multi-omics approach

To ensure that linkage disequilibrium was not responsible for the identified associations, we conducted an additional colocalization analysis. Lastly, we validated gene expression within prostate cancer tissue cells using single-cell sequencing analysis.

2.7 Ethics

All included studies received approval from their respective ethical review boards, and all participants provided signed consent.

2.8 Role of funders

The funding sources were not involved in the design of the study, data collection, analysis, interpretation, manuscript writing, or the decision to submit it for publication.

3 Results

3.1 Ribosome gene methylation and prostate cancer

Table 1 listed the causal effects of ribosome gene methylation on prostate cancer in McRae et al. methylation sequencing Cohort and Table 2 listed the causal effects in Hatton et al. methylation sequencing Cohort. Following the exclusion of associations with a P-HEIDI value below 0.01, 69 CpG sites located near 33 distinct genes met the nominal significance threshold ($P < 0.05$) in McRae et al. Cohort and a total of 131 CpG sites located close to 56 distinct genes met the threshold for nominal significance ($P < 0.05$) in Hatton et al. Cohort (Table S2). Among them, 50 CpG sites have an intersection between the two cohorts (Fig. S1 A). After correction for multiple testing (The Benjamini–Hochberg method), we identified 22 CpG sites near 9 unique genes in McRae et al. Cohort and 22 CpG sites near 9 unique genes in McRae et al. Cohort. In the McRae et al. Cohort, there were 17 near 4 unique genes were found to have strong colocalization evidence support (PPH4 > 0.70), including NSUN4 (cg00530320, cg00937489, cg02459555, cg04241075, cg06741803, cg08259313, cg10215817, cg12646227, cg13488501, cg14993813, cg15580309, cg17806798, cg17875957), LSM6 (cg27149555), GEMIN4 (cg19755813), EXOSC5 (cg01655341, cg05360949). In the Hatton et al. Cohort, there were 17 near 5 unique genes were found to have strong colocalization evidence support (PPH4 > 0.70), including ERI3 (cg03145482), ISG20L2 (cg05809481), NSUN4 (cg00530320, cg02459555, cg04241075, cg06741803, cg08259313, cg10215817, cg10495392, cg14993813, cg15580309, cg16553106, cg17806798, cg17875957), LSM6 (cg06372353, cg27149555), MPHOSPH6 (cg04290162). Interestingly, the results revealed the same gene different CpG sites effect direction were not always consistent which was observed in the NSUN4 gene. For instance, we found NSUN4 methylation site of cg10215817 was genetically associated with the increased risk of prostate cancer (OR 1.20, 95% confidence interval [CI] 1.10,1.30), while NSUN4 methylation site of cg00937489 was genetically associated with the decreased risk of prostate cancer (OR 0.84, 95% confidence interval [CI] 0.74,0.94). These results may reveal the complex gene regulation mechanism with occurrence of disease. Then, we validated the results is in the FinnGen population GWAS data (Table S3 and S4).

Table 1 Genetically predicted associations of ribosome gene methylations with prostate cancer (# McRae et al. Cohort)

Probe ID	Gene	Beta	SE	OR (95% CI)	P value	P value after FDR adjustment	P value (HEIDI test)	Number of SNPs used in HEIDI test	PPH4
cg00530320	NSUN4	0.082	0.020	1.09 (1.05, 1.13)	3.09E-05	0.002	0.450	20	0.811
cg00937489	NSUN4	− 0.179	0.050	0.84 (0.74, 0.94)	3.674E-04	0.009	0.326	4	0.825
cg02459555	NSUN4	0.122	0.036	1.13 (1.06, 1.20)	0.001	0.016	0.147	14	0.809
cg04241075	NSUN4	− 0.037	0.009	0.96 (0.94, 0.98)	1.16E-05	0.001	0.385	20	0.77
cg06741803	NSUN4	− 0.111	0.027	0.89 (0.84, 0.94)	4.03E-05	0.001	0.382	20	0.818
cg08259313	NSUN4	0.123	0.031	1.13 (1.07, 1.19)	8.01E-05	0.002	0.339	11	0.82
cg10215817	NSUN4	0.184	0.051	1.20 (1.10, 1.30)	3.397E-04	0.008	0.742	9	0.822
cg12646227	NSUN4	0.100	0.025	1.11 (1.06, 1.16)	4.35E-05	0.001	0.331	20	0.817
cg13488501	NSUN4	0.102	0.024	1.11 (1.06, 1.16)	3.16E-05	0.001	0.289	20	0.801
cg14993813	NSUN4	− 0.113	0.027	0.89 (0.84, 0.94)	3.90E-05	0.002	0.401	20	0.82
cg15580309	NSUN4	0.033	0.007	1.03 (1.02, 1.04)	7.95E-06	0.001	0.323	20	0.809
cg17806798	NSUN4	− 0.035	0.008	0.97 (0.95, 0.99)	1.11E-05	0.001	0.367	20	0.769
cg17875957	NSUN4	− 0.098	0.024	0.91 (0.86, 0.96)	4.10E-05	0.001	0.740	20	0.818
cg02196655	NOL10	0.086	0.012	1.09 (1.07, 1.11)	6.19E-13	0.000	0.084	20	0.0176
cg27149555	LSM6	0.051	0.014	1.05 (1.02, 1.08)	3.26E-04	0.008	0.376	20	0.703
cg00540449	MPHOSPH6	0.165	0.043	1.18 (1.10, 1.26)	1.03E-04	0.003	0.094	14	0.7
cg13294856	DDX52	0.110	0.036	1.12 (1.05, 1.19)	0.002	0.039	0.525	13	0.603
cg19755813	GEMIN4	− 0.185	0.044	0.83 (0.74, 0.92)	3.09E-05	0.002	0.172	5	0.996
cg12380854	MRPL10	− 0.111	0.036	0.89 (0.82, 0.96)	0.002	0.040	0.577	20	0.595
cg06146665	USP36	0.046	0.014	1.05 (1.02, 1.08)	0.001	0.022	0.471	20	0.575
cg01655341	EXOSC5	0.168	0.052	1.18 (1.08, 1.28)	0.001	0.024	0.128	5	0.951
cg05360949	EXOSC5	0.124	0.032	1.13 (1.07, 1.19)	1.20E-04	0.003	0.858	3	0.977

OR odds ratio, *CI* confidence interval, *PPH4* posterior probability of H4

Among these identified CpG sites, there were 5 sites were replicated, including cg27149555 near LSM6, cg05809481 near ISG20L2, cg06372353 near LSM6, cg04290162 near MPHOSPH6.

3.2 Ribosome gene splicing and prostate cancer

Table 3 present the results of causal effects of ribosome gene splicing on prostate cancer in Qi et al. splicing sequencing cohort and GTEx V8 cohort. There are a total of 74 splicing sites were found to have associations with prostate cancer at the nominally significant level threshold ($P < 0.05$) with P-HEIDI > 0.01 in the Qi et al. cohort and 14 splicing sites in the GTEx V8 cohort. After multiple testing correction and conducting colocalization analysis, genetically predicted splicing of MPHOSPH6 (site: chr16:82185119:82193842) (OR 1.09, 95% CI 1.05–1.14; PPH4 = 0.77), NOL10 (site: chr2:10784498:10797868) (OR 1.36, 95% CI 1.24–1.47; PPH4 = 0.807), NSUN4 (site: chr1:46340919:46341323) (OR 1.08, 95% CI 1.04–1.12; PPH4 = 0.813), NSUN4 (site: chr1:46341497:46344801) (OR 1.11, 95% CI 1.05–1.17; PPH4 = 0.824) were positively correlated with prostate cancer risk. In the contrary, genetically predicted splicing of LSM6 (site: chr4:147097495:147104064) (OR 0.87, 95% CI 0.79–0.95; PPH4 = 0.808), LSM6 (site: chr4:146175811:146182912) (OR 0.92, 95% CI 0.88–0.97; PPH4 = 0.808), NSUN4 (site: chr1:46340919:46344801) (OR 0.95, 95% CI 0.92–0.97; PPH4 = 0.82) were reversely correlated with prostate cancer risk (Tables 3 and 4). Interestingly, the results revealed the same gene different splicing sites effect direction were not always consistent which was observed in the NSUN4 gene again. (Table S5) Then, we replicated the results is in the FinnGen population (Table S6). Among these identified splicing sites, there were 5 sites were replicated, including LSM6 (chr4:147097495:147104064), MPHOSPH6 (chr16:82185119:82193842), NOL10 (chr2:10784498:10797868), NSUN4 (chr1:46341497:46344801).

Table 2 Genetically predicted associations of ribosome gene methylations with prostate cancer (# Hatton et al.)

Probe ID	Gene	Beta	SE	OR (95% CI)	P value	P value after FDR adjustment	P value (HEIDI test)	Number of SNPs used in HEIDI test	PPH4
cg03145482	ERI3	0.075	0.023	1.08 (1.03, 1.12)	0.001	0.030	0.870	11	0.767
cg00392257	ISG20L2	− 0.171	0.048	0.84 (0.75, 0.94)	3.42E-04	0.011	0.133	20	0.217
cg05809481	ISG20L2	− 0.213	0.065	0.81 (0.68, 0.94)	0.001	0.030	0.701	20	0.833
cg09507184	ISG20L2	− 0.228	0.074	0.80 (0.65, 0.94)	0.002	0.048	0.159	11	0.146
cg00530320	NSUN4	0.103	0.024	1.11 (1.06, 1.15)	1.55E-05	0.001	0.521	20	0.803
cg02459555	NSUN4	0.170	0.043	1.19 (1.10, 1.27)	7.41E-05	0.004	0.298	20	0.803
cg04241075	NSUN4	− 0.040	0.009	0.96 (0.94, 0.98)	1.07E-05	0.001	0.361	20	0.747
cg06741803	NSUN4	− 0.149	0.037	0.86 (0.79, 0.93)	5.64E-05	0.003	0.421	20	0.809
cg08259313	NSUN4	0.182	0.047	1.20 (1.11, 1.29)	1.00E-04	0.004	0.697	20	0.762
cg10215817	NSUN4	0.252	0.074	1.29 (1.14, 1.43)	0.001	0.019	0.774	14	0.804
cg10495392	NSUN4	0.064	0.015	1.07 (1.04, 1.09)	1.25E-05	0.001	0.426	20	0.789
cg14993813	NSUN4	− 0.091	0.021	0.91 (0.87, 0.96)	2.17E-05	0.001	0.293	20	0.784
cg15580309	NSUN4	0.033	0.007	1.03 (1.02, 1.05)	8.31E-06	0.001	0.273	20	0.790
cg16553106	NSUN4	− 0.167	0.041	0.85 (0.76, 0.93)	5.45E-05	0.003	0.618	20	0.794
cg17806798	NSUN4	− 0.036	0.008	0.96 (0.95, 0.98)	1.05E-05	0.001	0.448	20	0.782
cg17875957	NSUN4	− 0.117	0.028	0.89 (0.84, 0.94)	2.19E-05	0.001	0.796	20	0.805
cg02196655	NOL10	0.081	0.013	1.08 (1.06, 1.11)	6.29E-10	0.000	0.069	20	< 0.01
cg06372353	LSM6	− 0.032	0.009	0.97 (0.95, 0.99)	2.67E-04	0.009	0.567	20	0.713
cg27149555	LSM6	0.033	0.009	1.03 (1.02, 1.05)	3.09E-04	0.010	0.502	20	0.704
cg09893100	CHD7	− 0.128	0.042	0.88 (0.80, 0.96)	0.002	0.048	0.770	20	0.511
cg04290162	MPHOSPH6	− 0.290	0.078	0.75 (0.60, 0.90)	1.93E-04	0.008	0.117	20	0.714
cg01378812	DDX52	0.160	0.049	1.17 (1.08, 1.27)	0.001	0.030	0.087	20	< 0.01
cg07306685	DDX52	0.158	0.048	1.17 (1.08, 1.27)	0.001	0.031	0.211	20	< 0.01
cg13294856	DDX52	0.098	0.030	1.10 (1.04, 1.16)	0.001	0.030	0.061	20	0.416
cg06561728	GEMIN4	0.317	0.085	1.37 (1.21, 1.54)	2.01E-04	0.008	0.072	14	< 0.01
cg19755813	GEMIN4	− 0.255	0.065	0.77 (0.65, 0.90)	8.91E-05	0.004	0.064	20	< 0.01
cg12380854	MRPL10	− 0.076	0.021	0.93 (0.89, 0.97)	2.29E-04	0.008	0.133	20	< 0.01

OR odds ratio, *CI* confidence interval, *PPH4* posterior probability of H4

3.3 Ribosome gene expression and prostate cancer

Results for causal effects of ribosome gene expression on prostate cancer subtype are presented in Table 4 and Fig. 2E. In the eQTLGen cohort, a total of 25 ribosomal genes showed significant associations with prostate cancer ($P < 0.05$), meanwhile a total of 9 were identified in GTEx V8 cohort with P-HEIDI > 0.01 (Table S7). After multiple testing correction and conducting colocalization analysis, genetically predicted elevated genetically predicted expression levels of NSUN4 (OR 1.06, 95% CI 1.03–1.09; PPH4 = 0.79) and MPHOSPH6 (OR 1.07, 95% CI 1.04–1.10; PPH4 = 0.70) were positively associated with prostate cancer risk in eQTLGene cohort (Fig. 2A–D). In the GTEx V8 cohort, we found NSUN4 (OR 2.17, 95% CI 2.10–2.24; PPH4 = 0.757) was most significant correlation with prostate cancer. We replicated the results in the FinnGen study (Table S8). Expression levels of 29 ribosome-related genes were found to have nominally significant associations with prostate cancer ($P < 0.05$) in eQTLGene cohort with P-HEIDI > 0.01 including NSUN4. In GTEx V8, there are a total of 13 ribosome related gene expression were identified with $P < 0.05$ and P-HEIDI > 0.01. After multiple testing correction and conducting colocalization analysis, genetically predicted elevated levels expression of TP53 (OR 0.58, 95% CI 0.25–0.90) were negatively associated with prostate cancer risk and higher levels expression of MRM3 (OR 1.42, 95% CI 1.26–1.59) were positively associated with prostate cancer risk.

Discover Oncology (2025) 16:740 | https://doi.org/10.1007/s12672-025-02584-2

Table 3 Genetically predicted associations of ribosome gene splicing with prostate cancer (# Qi et al. and GTEx V8)

Probe ID	Gene	Beta	SE	OR (95% CI)	P value	P value after FDR adjustment	P value (HEIDI test)	Number of SNPs used in HEIDI test	PPH4
Qi et al. cohort									
chr4:147096963:147097320	LSM6	0.073	0.020	1.08 (1.04, 1.12)	3.50E-04	0.033	0.287	20	0.661
chr4:147097495:147104064	LSM6	− 0.141	0.040	0.87 (0.79, 0.95)	4.47E-04	0.038	0.559	19	0.808
chr4:147097589:147104064	LSM6	− 0.055	0.015	0.95 (0.92, 0.98)	3.52E-04	0.033	0.316	20	0.66
chr16:82185119:82193842	MPHOSPH6	0.090	0.022	1.09 (1.05, 1.14)	5.19E-05	0.008	0.012	20	0.772
chr2:10,784,498:10,797,868	NOL10	0.307	0.059	1.36 (1.24, 1.47)	1.89E-07	8.86E-05	0.525	20	0.807
GTEx V8 cohort									
chr4:146175811:146182912	LSM6	− 0.079	0.024	0.92 (0.88, 0.97)	0.001	0.038	0.273	6	0.71
chr1:46340919:46341323	NSUN4	0.080	0.020	1.08 (1.04, 1.12)	7.08E-05	0.005	0.576	15	0.813
chr1:46340919:46344801	NSUN4	− 0.055	0.013	0.95 (0.92, 0.97)	3.41E-05	0.003	0.599	20	0.82
chr1:46341497:46344801	NSUN4	0.106	0.030	1.11 (1.05, 1.17)	3.15E-04	0.016	0.333	6	0.824

Table 4 Genetically predicted associations of ribosome gene expression with prostate cancer (# eQTLGene and GTEx V8)

Gene	Beta	SE	OR (95% CI)	P value	P value after FDR adjustment	P value (HEIDI test)	PPH4
eQTLGene							
NSUN4	0.059	0.013	1.06 (1.03, 1.09)	1.01E-05	0.001	0.139	0.749
MTERF4	− 0.150	0.043	0.86 (0.78, 0.94)	4.39E-04	0.019	0.041	< 0.01
MPHOSPH6	0.068	0.014	1.07 (1.04, 1.10)	1.98E-06	2.59E-04	0.027	0.700
TP53	− 0.423	0.120	0.66 (0.42, 0.89)	4.08E-04	0.021	0.589	< 0.01
MRPL10	0.124	0.035	1.13 (1.06, 1.20)	3.71E-04	0.024	0.044	< 0.01
GTEx V8							
NSUN4	0.774	0.034	2.17 (2.10, 2.24)	1.67E-05	0.001	0.357	0.757

3.4 Cell-type specificity expression in the prostate tumor tissue

Through the integration of multi-omics results from SMR analysis, we identified two genes, NSUN4 and MPHOSPH6, supported by multi-omics data for their association with prostate cancer. To investigate potential cell type-specific enrichment of the genes coding for these two proteins within prostate cancer tissue, we conducted a single-cell expression analysis using RNA sequencing data from the GEO database. After integration and batch removal by harmony, there was no obvious batch effect among multiple groups of GSE221603; the samples in GSE221603 were divided into tumor group (01 T1, 01 T2, 02 T, 03 TA, 03 TB, 04 T1, 06 T, HSPC02, HSPC03) and normal group (01 N, 04 N, 06 N), and no obvious batch effect was observed between the two groups. (Fig. 3A) Cells were clustered into 12 clusters based on multiple cell markers (Fig. 3B) and were further classified into eight cell types (B cells, endothelial cells, epithelial cells, fibroblasts (cancer cells), mast cells, myeloid cells, neuroendocrine cells, T cells) (Fig. 3C). NSUN4 showed a higher expression in epithelial cells. In contrast, T cells and myeloid cells showed moderate expression levels. MPHOSPH6 presented a significantly higher expression in myeloid cells, but it was comparatively lower in epithelial and neuroendocrine cells (Fig. 3D).

4 Discussion

In this study, we performed SMR, colocalization, and single-cell sequencing to explore the associations of ribosome function and prostate cancer. We found that the ribosome-related genes *NSUN4* and *MPHOSPH6* were associated with prostate carcinoma with the most convincing multi-omics evidence.

NSUN4 encodes NOP2/Sun RNA Methyltransferase 4 (NSUN4), a dual-function protein that not only serves as an RNA m5 C methyltransferase, methylating C911 in 12S rRNA alone, but also regulates mitochondrial assembly [34–37]. *NSUN4* has been associated with multiple types of tumors. For example, it promotes hepatocellular carcinoma progression and serves as a prognostic indicator for this disease, and its mechanism is possibly related to methylation and demethylation [38, 39]. Furthermore, *NSUN4* methylation is linked with a reduced risk of breast cancer [19]. A study based on the TCGA database found that the expression level of NSUN4 in clear cell renal carcinoma was higher than that in normal tissues [40]. However, another similar study found that the increase in NSUN4 was associated with a better prognosis in renal clear cell carcinoma [41]. In a field related to this study, a MR analysis indicated that high expression of *NSUN4* is causally related to prostate cancer [19]. Additionally, genome-wide meta-analyses have identified *NSUN4* as a risk locus for prostate cancer at the 1p34 locus [42]. Analysis based on the KEGG database also found that NSUN4 is enriched in adherens junction signaling pathways [38]. And under hypoxic conditions, prostate cancer may secrete exosomes that modulate the expression of particular molecules in adherens junction related pathways, consequently enhancing cancer invasiveness [43]. *NSUN4* can upregulate CDC42 expression, which can consequently activate the PI3 K-AKT pathway and exert a pro-oncogenic effect [44]. The upregulation of *NSUN4* is also closely related to the p53 signaling pathway, the cell cycle signaling pathway, and the mTOR signaling pathway, suggesting that inhibitors or modulators targeting these pathways may influence its effects in cancer treatment [45]. A report showed that rapamycin can rescue the upregulation of the mTOR signaling pathway caused

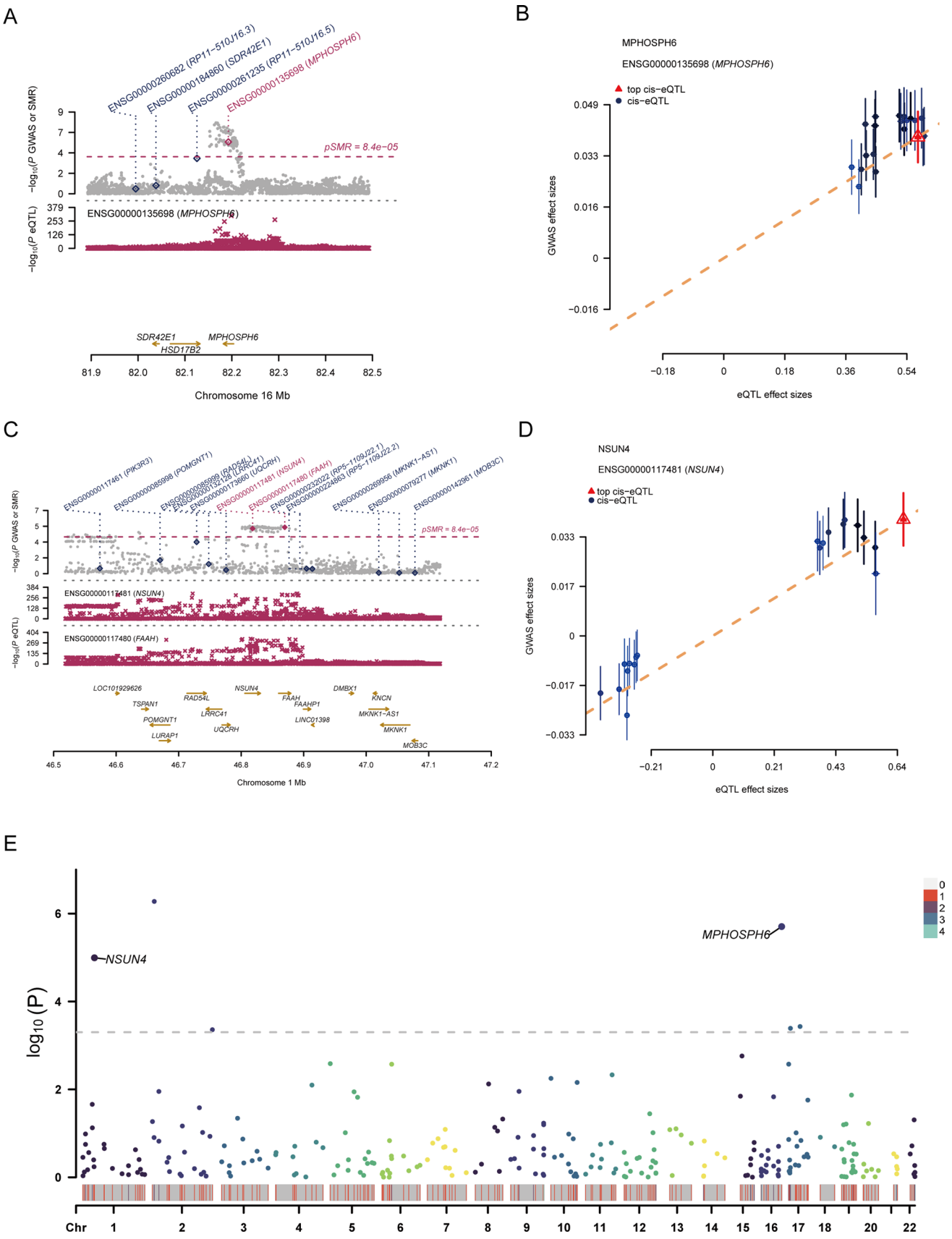

Fig. 2 SMR visualization and Manhattan Map. **A** Trajectory diagram of MPHOSPH6; **B** SMR plot of MPHOSPH6; **C** Trajectory diagram of NSUN4; **D** SMR plot of NSUN4; **E** Manhattan map of eQTL SMR results

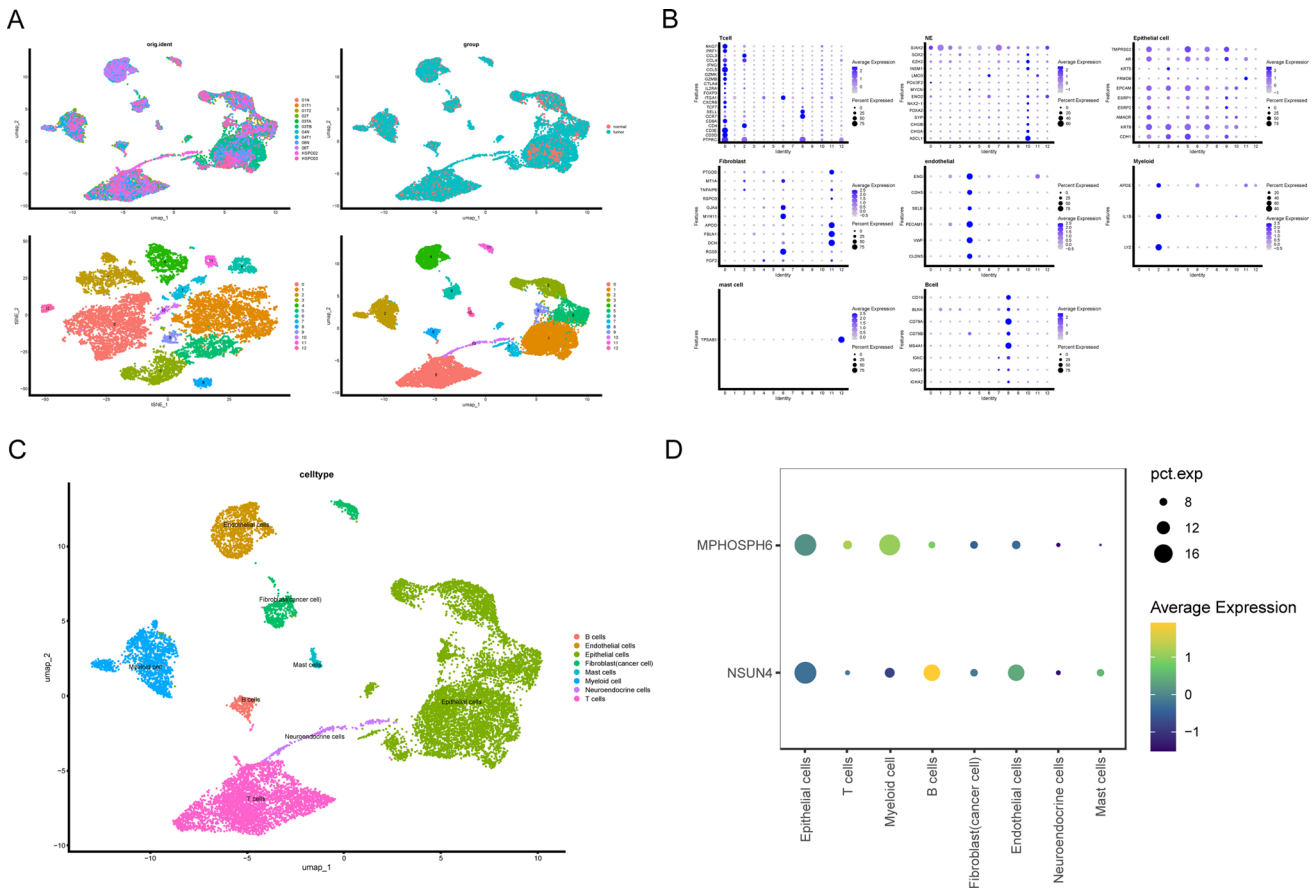

Fig. 3 Single cell sequencing results. **A** Integration and batch removal by harmony; samples were divided into tumor group and normal group; resolution 0.1, tSNA algorithm dimensionality reduction clustering; resolution 0.1, UMAP algorithm dimensionality reduction clustering. **B** Characteristic expression of various cell markers in 8 types of cells (B cells, Endothelial cells, Epithelial cells, Fibroblast cells, Mast cells, Myeloid cells, Neuroendocrine cells, T cells). **C** UMAP visualization of cell clusters from a single-cell analysis. **D** Expression of NSUN4 and MPHOSPH6 across different cell types

by *NSUN4* overexpression, thereby slowing down tumor development [46]. However, limited research has been conducted that focused on *NSUN4* and prostate cancer from observational epidemiological and experimental perspectives. In our study, we found that high expression of *NSUN4* correlates with an increased risk of prostate cancer, suggesting a causal link. Intriguingly, methylation or splicing at different loci exhibited completely opposite effects on prostate cancer risk. A possible explanation to the non-uniform regulatory effects of the methylation would be the distinct functional roles of different sites. For instance, certain CpG sites within a gene promoter region are often associated with transcriptional repression when methylated, while methylation within the gene body can enhance transcriptional elongation and stability of the mRNA transcript [47, 48]. However, there were few research on the *NSUN4* methylation or splicing of prostate cancer, suggesting a need for further fundamental research into this gene's complex mechanisms.

Another ribosome-related gene identified by our study is *MPHOSPH6*. It encodes M-phase phosphoprotein 6 (MPHOSPH6), which is a specific exosomal cofactor from the nucleolus, and is essential for the maturation of 5.8S rRNA [49]. This gene has also been linked to various tumors. A Mendelian randomization study indicates that elevated expression of *MPHOSPH6* is associated with an increased risk of lung cancer [50]. Furthermore, database analyses suggest a correlation between *MPHOSPH6* and ovarian cancer, potentially through its involvement in niacin and nicotinamide metabolism, the spliceosome, thyroid hormone signaling pathways, the cell cycle, and glucagon signaling pathways [50]. Additionally, genetic association studies have demonstrated a positive correlation between variations in *MPHOSPH6* and susceptibility to hepatocellular carcinoma, with abnormal cell division implicated as a possible mechanism [51]. In a study based on The Cancer Genome Atlas data, *MPHOSPH6* was lowly expressed in prostate adenocarcinoma, however, the overall survival of patients in the high expression group was much shorter than that of patients in the low expression

group [52]. Our MR analysis further substantiates that high expression and splicing of the *MPHOSPH6* gene elevate the risk of prostate cancer. Further epidemiological and experimental studies are needed to confirm our findings.

The strengths of this study are as follows. First, SMR and single cell sequencing were employed to investigate the relationship between ribosome-related genes and prostate cancer, somewhat strengthening the causal link between these genes and prostate cancer. MR can address the issues of confounding bias and reverse causality in observational studies. Second, a large number of GWAS results were utilized to carry out MR analysis, enhancing statistical power. Moreover, we applied multi-omics approaches, utilizing SMR and colocalization analysis for a combined analysis to mitigate horizontal pleiotropy, and using single-cell sequencing to validate the findings. The methods significantly enhanced the robustness of the study. However, this study has several limitations. In this research, the observed genetic variation linked to the ribosomal genome predominantly originated from nuclear DNA associated with ribosomal functions, rather than the ribosomal genome directly, owing to the absence of a ribosomal genome-specific QTL dataset. Despite performing various sensitivity analyses to validate the assumptions of the MR framework, we cannot fully exclude the potential for confounding bias or horizontal pleiotropy. Cell and animal experiments are needed to further validate the findings. Moreover, the GWAS and QTL data employed were primarily sourced from European ancestry populations, which may limit the generalizability of our findings to other geographic and ethnic groups. The applicability of these findings to other populations needs to be further confirmed by future research using non-European ancestry databases. Last, we evaluated the expression of genes in prostate cancer, but were unable to estimate the levels of related proteins in other tissues. Further assessing the role of protein levels in other tissues in prostate cancer may provide a deeper understanding of its pathogenesis.

This research investigated the potential causal links between prostate cancer and ribosome-related gene methylation, splicing, and expression through SMR, co-localization, and single-cell sequencing. These results enhance our comprehension of the underlying pathological mechanism of prostate cancer and may reveal potential pharmacological targets related to tumor prevention or treatment.

Acknowledgements Not applicable.

Author contributions Chengcheng Wei and Jingke He: Conceptualization, Data curation, Formal analysis, Methodology, Software, Visualization, Writing—original draft, Writing—review & editing. Yunfan Li and Yu Luo: Conceptualization, Methodology, Writing—review & editing. Liangdong Song and Kun Han: Validation, Writing—review & editing. Jindong Zhang, Shuai Su and Delin Wang: Conceptualization, Funding acquisition, Methodology, Supervision, Writing—review & editing.

Funding Not applicable.

Data availability Data is provided within the manuscript or supplementary information files.

Declarations

Competing interests The authors declare no competing interests.

References

1. Siegel RL, Giaquinto AN, Jemal A. Cancer statistics, 2024. CA Cancer J Clin. 2024;74(1):12–49.
2. Bray F, et al. Global cancer statistics 2022: GLOBOCAN estimates of incidence and mortality worldwide for 36 cancers in 185 countries. CA Cancer J Clin. 2024;74(3):229–63.
3. Mathis AD, et al. Mechanisms of in vivo ribosome maintenance change in response to nutrient signals. Mol Cell Proteomics. 2017;16(2):243–54.
4. Chakraborty A, et al. Loss of ribosomal protein L11 affects zebrafish embryonic development through a p53-dependent apoptotic response. PLoS ONE. 2009;4(1): e4152.

5. Rao S, et al. Inactivation of ribosomal protein L22 promotes transformation by induction of the stemness factor, Lin28B. Blood. 2012;120(18):3764–73.
6. Yang M, et al. Interaction of ribosomal protein L22 with casein kinase 2α: a novel mechanism for understanding the biology of non-small cell lung cancer. Oncol Rep. 2014;32(1):139–44.
7. Zhao PY, et al. Eukaryotic ribosome quality control system: a potential therapeutic target for human diseases. Int J Biol Sci. 2022;18(6):2497–514.
8. Hernández G, et al. The secret life of translation initiation in prostate cancer. Front Genet. 2019;10:14.
9. Lawrence MG, et al. Patient-derived models of abiraterone- and enzalutamide-resistant prostate cancer reveal sensitivity to ribosome-directed therapy. Eur Urol. 2018;74(5):562–72.
10. Wang M, Hu Y, Stearns ME. RPS2: a novel therapeutic target in prostate cancer. J Exp Clin Cancer Res. 2009;28(1):6.
11. Koutsougianni F, et al. P90 ribosomal S6 kinases: a bona fide target for novel targeted anticancer therapies? Biochem Pharmacol. 2023;210:115488.
12. Cronin R, Brooke GN, Prischi F. The role of the p90 ribosomal S6 kinase family in prostate cancer progression and therapy resistance. Oncogene. 2021;40(22):3775–85.
13. Ushijima M, et al. An oral first-in-class small molecule RSK inhibitor suppresses AR variants and tumor growth in prostate cancer. Cancer Sci. 2022;113(5):1731–8.
14. Ding M, et al. SIRT7 depletion inhibits cell proliferation and androgen-induced autophagy by suppressing the AR signaling in prostate cancer. J Exp Clin Cancer Res. 2020;39(1):28.
15. Lagunas-Rangel FA. The dark side of SIRT7. Mol Cell Biochem. 2023. https://doi.org/10.1007/s11010-023-04869-y.
16. Fenner A. Prostate cancer: targeting the ribosome in advanced disease. Nat Rev Urol. 2016;13(10):562.
17. Emdin CA, Khera AV, Kathiresan S. Mendelian randomization. JAMA. 2017;318(19):1925–6.
18. Davies NM, Holmes MV, Davey Smith G. Reading Mendelian randomisation studies: a guide, glossary, and checklist for clinicians. Bmj. 2018;362:601.
19. Li Y, et al. Mitochondrial related genome-wide Mendelian randomization identifies putatively causal genes for multiple cancer types. EBioMedicine. 2023;88:104432.
20. Han H, et al. Identifying MTHFD1 and LGALS4 as potential therapeutic targets in prostate cancer through multi-omics Mendelian randomization analysis. Biomedicines. 2025. https://doi.org/10.3390/biomedicines13010185.
21. Oliva M, et al. DNA methylation QTL mapping across diverse human tissues provides molecular links between genetic variation and complex traits. Nat Genet. 2023;55(1):112–22.
22. Hatton AA, et al. Genetic control of DNA methylation is largely shared across European and East Asian populations. Nat Commun. 2024;15(1):2713.
23. Wu Y, et al. Integrative analysis of omics summary data reveals putative mechanisms underlying complex traits. Nat Commun. 2018;9(1):918.
24. McRae AF, et al. Identification of 55,000 replicated DNA methylation QTL. Sci Rep. 2018;8(1):17605.
25. Qi T, et al. Genetic control of RNA splicing and its distinct role in complex trait variation. Nat Genet. 2022;54(9):1355–63.
26. Consortium G. The GTEx consortium atlas of genetic regulatory effects across human tissues. Science. 2020;369(6509):1318–30.
27. Võsa U, et al. Large-scale cis- and trans-eQTL analyses identify thousands of genetic loci and polygenic scores that regulate blood gene expression. Nat Genet. 2021;53(9):1300–10.
28. Zang Y, et al. Genomic hallmarks and therapeutic targets of ribosome biogenesis in cancer. Brief Bioinform. 2024. https://doi.org/10.1093/bib/bbae023.
29. Nerurkar P, et al. Eukaryotic ribosome assembly and nuclear export. Int Rev Cell Mol Biol. 2015;319:107–40.
30. Schumacher FR, et al. Association analyses of more than 140,000 men identify 63 new prostate cancer susceptibility loci. Nat Genet. 2018;50(7):928–36.
31. Kurki MI, et al. FinnGen provides genetic insights from a well-phenotyped isolated population. Nature. 2023;613(7944):508–18.
32. Zhu Z, et al. Integration of summary data from GWAS and eQTL studies predicts complex trait gene targets. Nat Genet. 2016;48(5):481–7.
33. Dashti HS, et al. Genetic determinants of daytime napping and effects on cardiometabolic health. Nat Commun. 2021;12(1):900.
34. Spåhr H, et al. Structure of the human MTERF4-NSUN4 protein complex that regulates mitochondrial ribosome biogenesis. Proc Natl Acad Sci USA. 2012;109(38):15253–8.
35. Yakubovskaya E, et al. Structure of the essential MTERF4:NSUN4 protein complex reveals how an MTERF protein collaborates to facilitate rRNA modification. Structure. 2012;20(11):1940–7.
36. Cámara Y, et al. MTERF4 regulates translation by targeting the methyltransferase NSUN4 to the mammalian mitochondrial ribosome. Cell Metab. 2011;13(5):527–39.
37. Metodiev MD, et al. NSUN4 is a dual function mitochondrial protein required for both methylation of 12S rRNA and coordination of mitoribosomal assembly. PLoS Genet. 2014;10(2):11.
38. Cui MX, et al. m5C RNA methyltransferase-related gene NSUN4 stimulates malignant progression of hepatocellular carcinoma and can be a prognostic marker. Cancer Biomark. 2022;33(3):389–400.
39. He Y, et al. Role of m(5)C-related regulatory genes in the diagnosis and prognosis of hepatocellular carcinoma. Am J Transl Res. 2020;12(3):912–22.
40. Li H, et al. Prognostic value of an m(5)C RNA methylation regulator-related signature for clear cell renal cell carcinoma. Cancer Manag Res. 2021;13:6673–87.
41. Wu J, et al. Comprehensive analysis of m(5)C RNA methylation regulator genes in clear cell renal cell carcinoma. Int J Genomics. 2021;2021:3803724.
42. Kar SP, et al. Genome-wide meta-analyses of breast, ovarian, and prostate cancer association studies identify multiple new susceptibility loci shared by at least two cancer types. Cancer Discov. 2016;6(9):1052–67.
43. Ramteke A, et al. Exosomes secreted under hypoxia enhance invasiveness and stemness of prostate cancer cells by targeting adherens junction molecules. Mol Carcinog. 2015;54(7):554–65.

44. Zhao Z, et al. NSUN4 mediated RNA 5-methylcytosine promotes the malignant progression of glioma through improving the CDC42 mRNA stabilization. Cancer Lett. 2024;597:217059.
45. Pan J, Huang Z, Xu Y. m5C RNA methylation regulators predict prognosis and regulate the immune microenvironment in lung squamous cell carcinoma. Front Oncol. 2021;11:657466.
46. Wang C, et al. NOP2/Sun RNA methyltransferase 4 regulates the mammalian target of rapamycin signaling pathway to promote hepatocellular carcinoma progression. Turk J Gastroenterol. 2024;36(1):24–33.
47. Ogushi S, et al. CpG site-specific regulation of metallothionein-1 gene expression. Int J Mol Sci. 2020. https://doi.org/10.3390/ijms21175946.
48. De S, et al. Aberration in DNA methylation in B-cell lymphomas has a complex origin and increases with disease severity. PLoS Genet. 2013;9(1):e1003137.
49. Schilders G, et al. MPP6 is an exosome-associated RNA-binding protein involved in 5.8S rRNA maturation. Nucleic Acids Res. 2005;33(21):6795–804.
50. Cortez Cardoso Penha R, et al. Common genetic variations in telomere length genes and lung cancer: a Mendelian randomisation study and its novel application in lung tumour transcriptome. Elife. 2023. https://doi.org/10.7554/eLife.83118.
51. Zhang Y, et al. Association of ACYP2 and MPHOSPH6 genetic polymorphisms with the risk of hepatocellular carcinoma in chronic hepatitis B virus carriers. Oncotarget. 2017;8(49):86011–9.
52. Huang H, et al. Zinc finger C3H1 domain-containing protein (ZFC3H1) evaluates the prognosis and treatment of prostate adenocarcinoma (PRAD): a study based on TCGA data. Bioengineered. 2021;12(1):5504–15.